RAA 2021 Vol. **21** No. **4**, 105(6pp) doi: 10.1088/1674-4527/21/4/105
© 2021 National Astronomical Observatories, CAS and IOP Publishing Ltd.
http://www.raa-journal.org *http://iopscience.iop.org/raa*

***R**esearch in*
***A**stronomy and*
***A**strophysics*

Observation of solar coronal heating powered by magneto-acoustic oscillations in a moss region

Parida Hashim[1,2], Zhen-Xiang Hong[3], Hai-Sheng Ji[3,4], Jin-Hua Shen[2], Kai-Fan Ji[5] and Wen-Da Cao[6]

[1] Graduate School of the Chinese Academy of Sciences, Beijing 100871, China
[2] Xinjiang Astronomical Observatory, Chinese Academy of Sciences, Urumqi 830011, China
[3] Purple Mountain Observatory, DMSA/CAS, Nanjing 210023, China; *jihs@pmo.ac.cn*
[4] CfASS, China Three Gorges University, Yichang 443002, China
[5] Yunnan Astronomical Observatory, Chinese Academy of Sciences, Kunming 830011, China
[6] Big Bear Solar Observatory, 40386 North Shore Lane, Big Bear City, CA 922314, USA

Received 2020 July 27; accepted 2020 September 6

Abstract In this paper, we report the observed temporal correlation between extreme-ultraviolet (EUV) emission and magneto-acoustic oscillations in an EUV moss region, which is the footpoint region only connected by magnetic loops with million-degree plasma. The result is obtained from a detailed multi-wavelength data analysis of the region with the purpose of resolving fine-scale mass and energy flows that come from the photosphere, pass through the chromosphere and finally heat the solar transition region or the corona. The data set covers three atmospheric levels on the Sun, consisting of high-resolution broad-band imaging at TiO 7057 Å and the line of sight magnetograms for the photosphere, high-resolution narrow-band images at helium I 10830 Å for the chromosphere and EUV images at 171 Å for the corona. The 10830 Å narrow-band images and the TiO 7057 Å broad-band images are from a much earlier observation on 2012 July 22 with the 1.6 meter aperture Goode Solar Telescope (GST) at Big Bear Solar Observatory (BBSO) and the EUV 171 Å images and the magnetograms are from observations made by Atmospheric Imaging Assembly (AIA) or Helioseismic and Magnetic Imager (HMI) onboard the Solar Dynamics Observatory (SDO). We report the following new phenomena: (1) Repeated injections of chromospheric material appearing as 10830 Å absorption are squirted out from inter-granular lanes with a period of ~ 5 minutes. (2) EUV emissions are found to be periodically modulated with similar periods of ~ 5 minutes. (3) Around the injection area where 10830 Å absorption is enhanced, both EUV emissions and strength of the magnetic field are remarkably stronger. (4) The peaks on the time profile of the EUV emissions are found to be in sync with oscillatory peaks of the stronger magnetic field in the region. These findings may give a series of strong evidences supporting the scenario that coronal heating is powered by magneto-acoustic waves.

Key words: Sun: corona — Sun: chromosphere — Sun: magnetic field

1 INTRODUCTION

A fundamental and long standing problem in astrophysics is why the tenuous solar (and many stellar) corona has a million-degree temperature far in excess of the underlying vastly denser photosphere. More and more evidence has revealed that the heating energy is generated directly from the photosphere via hot expulsions, spicules or Alfvén waves (McIntosh et al. 2011; Tian et al. 2014; Peter et al. 2014; Dinesh Singh & Singh Jatav 2019), but leaving no residual traces on it. Resolution of this problem ultimately relies on resolving fine-scale mass and energy flows passing through the chromosphere, the interface layer sandwiched between the photosphere and the transition region or the corona (De Pontieu et al. 2014; Tian 2017; De Pontieu et al. 2009; Aschwanden et al. 2007).

By exploring correlations between the oscillatory signals observed at different levels of the solar atmosphere, much progress has been made on resolving the mass and energy flows passing through the chromosphere, the interface layer (De Pontieu et al. 2014, 2009; Aschwanden et al. 2007). On the other hand, helium I 10830 Å narrow-band imaging has proven to be one of the best tools for precisely tracking mass and energy flows from below (Ji et al. 2012; Hong et al. 2017). The helium I 10830 Å line is a weak absorption line seen against the solar disk, yet the line is so special that the chromospheric line is associated with excitation by high-energy extreme-

ultraviolet (EUV) photons. So, it is a line formed in the upper chromosphere. Since the line is shallow, a narrow-band filtergram at this line taken near the disk center contains the features of the photosphere like granules. Therefore, a big and crucial advantage for a narrow-band filtergram taken at this line is that it can be precisely aligned with simultaneous images of the photosphere.

Over the solar disk, the coronal heating rate differs at different parts of the solar surface, ranging from active regions to coronal holes. An important target for studying the interface layer is footpoint regions of coronal loops, appearing as faculae on the photosphere or plages in the chromosphere (Li & Ding 2009). The region is believed to have a stronger heating rate, with prevalent oscillations at various wavebands (De Pontieu et al. 2003). In a plage area, of particular interest is the so-called EUV "moss", a region being connected to coronal loops with million-degree hot plasma. In this region, much stronger heating rate is believed to be constantly occurring. Nevertheless, the region has its name since it is full of dark inclusions from low temperature plasma making it take the appearance of reticulated bright EUV emission (Berger et al. 1999; Fletcher & De Pontieu 1999). The dark inclusions are found to jointly appear and disappear, a signature of oscillatory fine-scale mass and energy flows rising upward (Fletcher & De Pontieu 1999; De Pontieu et al. 2003; De Pontieu & Erdélyi 2006). On the other hand, the oscillatory emissions of coronal loops as well as the rooted footpoint regions usually serve as indirect evidences of magneto-acoustic waves (Jess et al. 2015; Banerjee et al. 2007; Nakariakov & Verwichte 2005). The heating of the corona or plasma via damping of magneto-acoustic waves is of great interest across the entire community of astrophysics, as well as the plasma physics community (Stix 1975; Kolotkov et al. 2019). However, as the first step, reliable correlations between the heating and magneto-acoustic oscillations have to be determined spatiotemporally with solid observations.

On 2012 July 22 high-resolution narrow-band imaging at helium I 10830 Å for the chromosphere and broad-band imaging at TiO 7057 Å lines for the photosphere were carried out, targeting the active region NOAA 11259 (Ji et al. 2012, JCG12 hereafter). The observations have revealed the smallest scale magnetic activities in inter-granular lanes of the photosphere with their brightening going up into the local transition region. The finding was confirmed by further analysis of the same data set or similar observations (Zeng et al. 2013; Hong et al. 2017; Yang et al. 2019). In the most recent work, Ji et al. (2021) reported a possible correlation between the perturbations of magnetic field and He I 10830 Å absorption, and both have a quasi-periodic nature. In the paper, they switch to concentrate on demonstrating that the magnetic field perturbations are magneto-acoustic oscillations powered by p-mode. In this paper, we conduct a thorough analysis of the correlation. We report on the peak-to-peak correlations between EUV emissions and magneto-acoustic oscillations. Observational results are given in Section 2 and conclusions are provided in Section 3.

2 OBSERVATIONAL RESULTS

For details on the observations, we guide readers to the paper JCG12. In this section, we will directly introduce the results analyzed from the observations. We feature Figure 1 here to show the observations made by different instruments. It includes the EUV moss region (the area of interest: AOI), its surrounding plages and the active region. The EUV moss region, with an area of 10 Mm $\times$ 10 Mm, is inside the chartreuse-colored boxes in all panels (Fig. 1(a)-(d). Figure 1(a) and 1(c) depicts the EUV observation made by Atmospheric Imaging Assembly (AIA) at Fe IX 171 Å onboard Solar Dynamics Observatory (SDO) and the X-ray telescope (XRT) onboard Hinode taken with the Ti-poly filter (Kosugi et al. 2007; Golub et al. 2007). In Figure 1(d) we specially give a larger field of view to display the morphology of the active region and its position on the solar disk. A moss region is usually situated at footpoints of soft X-ray (SXR) loops of million-degree plasma (Berger et al. 1999; Fletcher & De Pontieu 1999), so it is an ideal place for investigating the problem of coronal heating. A line-of-sight magnetogram observed by the Helioseismic and Magnetic Imager (HMI) (Schou et al. 2012) onboard SDO (Pesnell et al. 2012) is given to demonstrate the magnetic nature of the moss region (Fig. 1(c)). The magnetic field has negative polarity, so we will use an unsigned magnetic field for research in this paper.

Panel (b) gives high-resolution imaging at narrow-band helium I 10830 Å for the region. The high-resolution reveals many small scale, and thus ubiquitous, upward mass injections in the form of enhanced 10830 Å absorption patches (EAPs), as defined and discussed by Hong et al. (2017). From panel (a), we can see that point-like EUV dark inclusions from low temperature plasma are in the midst of EUV emissions. Dark inclusions are actually cool material being squirted upward as mass injections (Berger et al. 1999; Fletcher & De Pontieu 1999). As we will see in this paper, the dark inclusions, together with EUV emission, are spatiotemporally associated with enhanced helium I 10830 Å absorptions. The phenomenon signifies that the dark inclusions or enhanced helium I 10830 Å absorptions are accompanied by some kind of heating processes. In panel (b), an enlargement of the ROI is specially given to showcase the EAPs at 10830 Å, which is within the contour level of 4.6×10^3 counts pixel^{-1}. We call other areas less 10830 Å absorption patches (LAPs). For the purpose of subsequent statistics, the value of 4.6×10^3 counts pixel^{-1} is chosen in such a way that its contour level divides the ROI into two regions with roughly equal areas. The value corresponds to $\sim$ 95% of the average band pass intensity for the moss region.

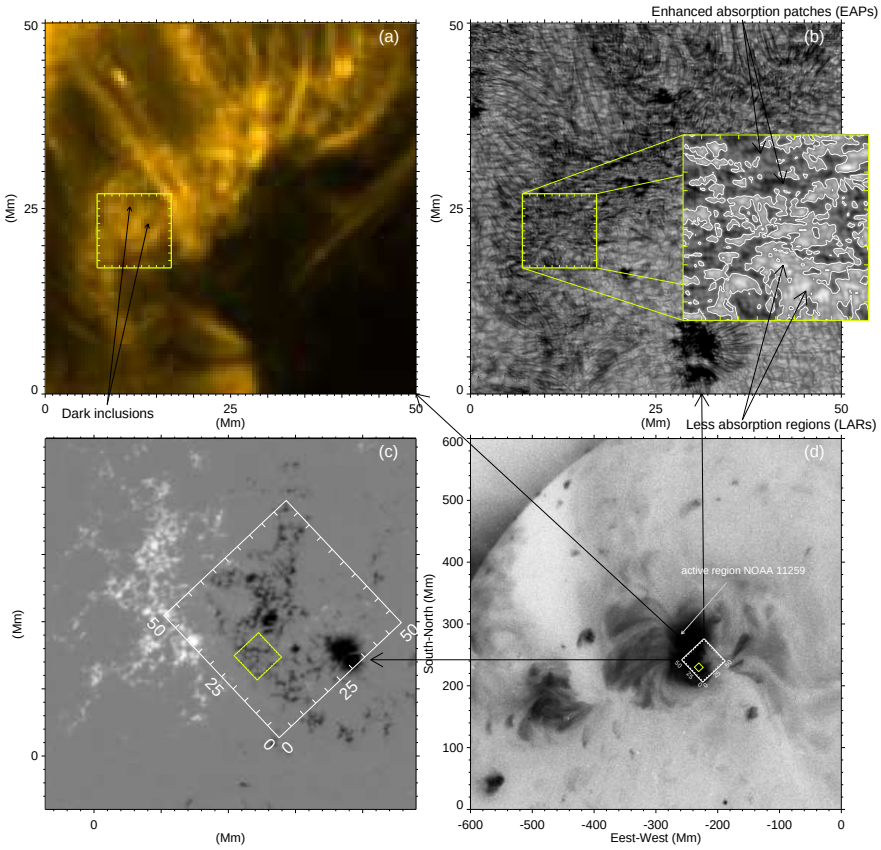

Fig. 1 The chartreuse-colored boxes in all panels outline the site of the EUV moss region with an area of 10 Mm $\times$ 10 Mm. Panels (a)-(c) display the images at Fe IX 171 Å observed by AIA, helium I 10830 Å observed by GST and a line-of-sight magnetogram observed by HMI, respectively. In panel (b), an enlargement for the AOI is specially featured to show EAPs and the patches with LAPs. The EAPs are defined as darkened areas within the contour level of 4.5×10^3 counts pixel^{-1}. Panel (d), with a larger field of view, features an SXR image taken with the Ti-poly filter by the XRT onboard Hinode.

As can be seen from the online animation in the paper JCG12, there are numerous upward injections of helium I 10830 Å absorption material in the plage region. The injections actually repeat themselves in the same place periodically. The periodical nature can be demonstrated with a time-distance diagram made of a straight line across the area. Figure 2-C2 features a sample time-distance diagram at 10830 Å from which we can see rows of periodical absorption structures. To ascertain their spatial information on the photosphere, Figure 2-A2 gives a time-distance diagram for the photosphere made of a vertical slice in the same place. On the time-distance diagram, inter-granular lanes exhibit similar rows of parallel structures. The combination of the two kinds of time-distance diagrams composed of helium I 10830 Å and TiO 7057 Å images confirms that the mass injections are coming out of inter-granular lanes, or the boundaries of solar granules (Fig. 2-B2 or S2.mp4). The associated EUV brightening manifests a similar periodic structure which we have just described. It is also worth noting that the rows of structures in the three time-distance diagrams (C2, B2 and D2) exhibit similar moving patterns in the online animation. This phenomenon represents additional evidence demonstrating that the mass injections come out of inter-granular lanes.

In the same place sandwiched between the two dark parallel lines (Fig. 2-C2 and D2), we cut two slices out of the I 10830 Å and EUV 171 Å time-distance diagrams and covert them into two light curves. They are displayed in Figure 3(a) and (c). Wavelet analysis of the light curves yields the oscillation period in the right two panels. They both have a component of $\sim$ 5 minutes, showing that they are somehow affected by the p-mode oscillation. We see that EUV emissions are correlated with the 10830 Å absorption in a much more complex manner. The material injections from below, shown as EAPs, make contributions to dark inclusions. However, as we will see, they do heat the transition region to enhance EUV brightening at the same time.

Figure 4(a) plots mean EUV emission at 171 Å averaged over EAPs and LAPs in the moss region. We see that the EUV emission over the EAPs, traced with a red light curve, is systematically more intense over the region of EAPs. Emissions in other EUV wavelengths have

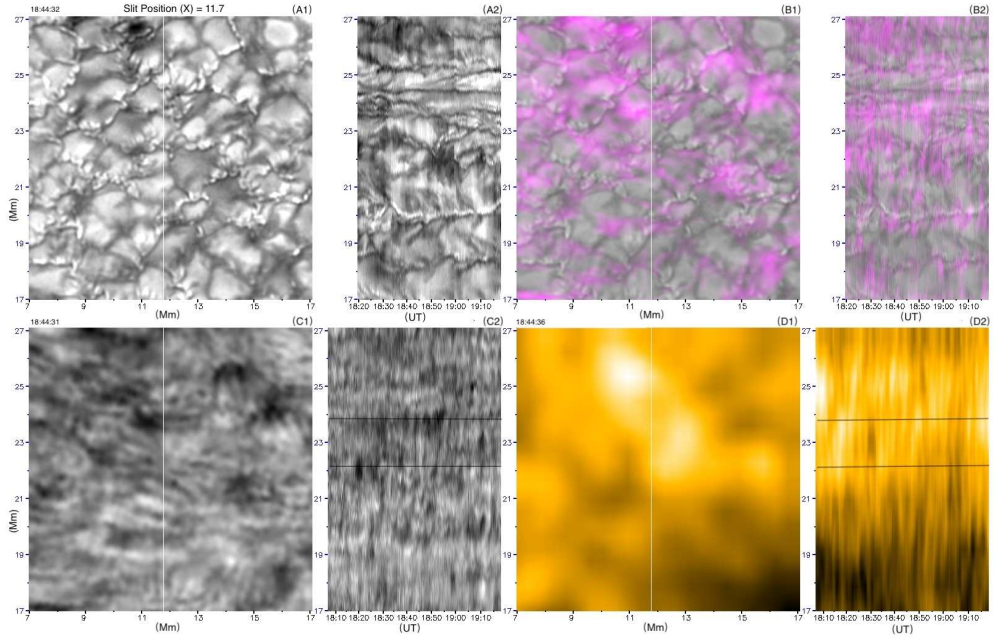

Fig. 2 Panel A1 depicts the photosphere in the moss region as observed with a broad-band (10 Å) filter at TiO 7057 Å by GST (18:44:32 UT). Panels C1-D1 are the images of the moss region at helium I 10830 Å (18:44:31 UT) and Fe IX 171 Å (18:44:36 UT) respectively. Panel (B1) displays a composite image generated by taking the photospheric emission as background and putting 10830 Å absorption (in *pink*) over it. Panels (A1-D1) have the same field of view (10×10 Mm^2) as the chartreuse-colored boxes in Fig. 1. Panels (A2-D2) give four time-distance diagrams generated from the intensity distribution of the corresponding images along the vertical slit (the position of the vertical slit for this figure is at 11.4 Mm) shown in panels (A1-D1). The two sets of dark parallel lines are the boundaries of two slices being cut to become time profiles in Fig. 3(a) and (c). Online animation for varying time-distance diagrams generated with different slit positions is available.

a similar behavior (Hong et al. 2017). We also compare strength of the magnetic field in the EAPs and LAPs and the result implies that mean magnetic field is also systematically more intense over the region of EAPs (Fig. 4(b)). Furthermore, the two kinds of time profiles seem to have a kind of peak-to-peak correlation, when we compare the perturbations on the light curves. To exclude the possibility that the temporal variations of mean magnetic field in Figure 4(b) may be affected by the area of EAPs, which are also periodically changing, we computed another kind of time profile for the mean magnetic field for the region with the stronger field. For a certain time (say at 18:42:41 UT in this analysis), we select those pixels where the unsigned magnetic field is larger than 250 G. Then these pixels are collected together and get fixed to produce the time profile in Figure 4(c). We see that the peak-to-peak correspondence still exists with the exception of a few EUV peaks. With the help of a series of vertical lines in Figure 4, we see that 14 out of the 18 EUV peaks can be regarded as being well correlated with the peaks of magnetic field perturbations.

3 DISCUSSION AND CONCLUSIONS

High-resolution 10830 Å narrow-band images are actually composite images containing dual features of the upper chromosphere and the photosphere. There are numerous photospheric features which enable us to align the 10830 Å narrow-band images with the images of the photosphere at TiO 7057 Å with unprecedented precision. It can be called a natural co-alignment. Therefore, we can pin down the features of the chromosphere, 10830 Å absorption in this paper, on the photosphere with least ambiguity. The precise co-alignment for high-resolution images has yielded the finding of magnetic activities in inter-granular lanes driven by granular convections (JCG12; Zeng et al. 2013; Hong et al. 2017). It is worth mentioning that, with high-resolution spectroscopic imaging in He I 10830 Å, Yang et al. (2019) reported that plasma flows along the magnetic loops are ejected from and drained out into inter-granule lane areas at different ends of magnetic loops.

With the same set of data as being observed and analyzed by JCG12, the paper aims to resolve fine-scale mass and energy flows in the chromosphere and their role in heating the corona. The mass and energy flows are signified by the periodic mass injections seen as 10830 Å absorption in the selected moss region. For the periodic mass injections, they may also be the on-disk counterparts of spicules. For these periodic mass injections, we can conclude that

– They have a period of $\sim$ 5 minutes,

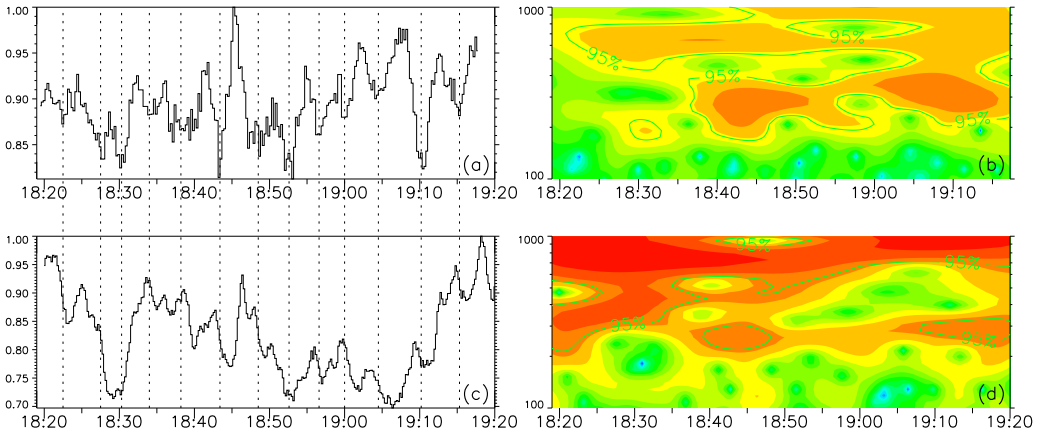

Fig. 3 Left two panels plot two time profiles that are obtained from the rebinning of two slice time-distance diagrams featured in Fig. 2. The result of their wavelet analysis is displayed in the right two panels. The upper two panels are for 10830 Å while the lower two panels are for 171 Å. Vertical dashed lines indicate the times of the strongest 10830 Å absorption.

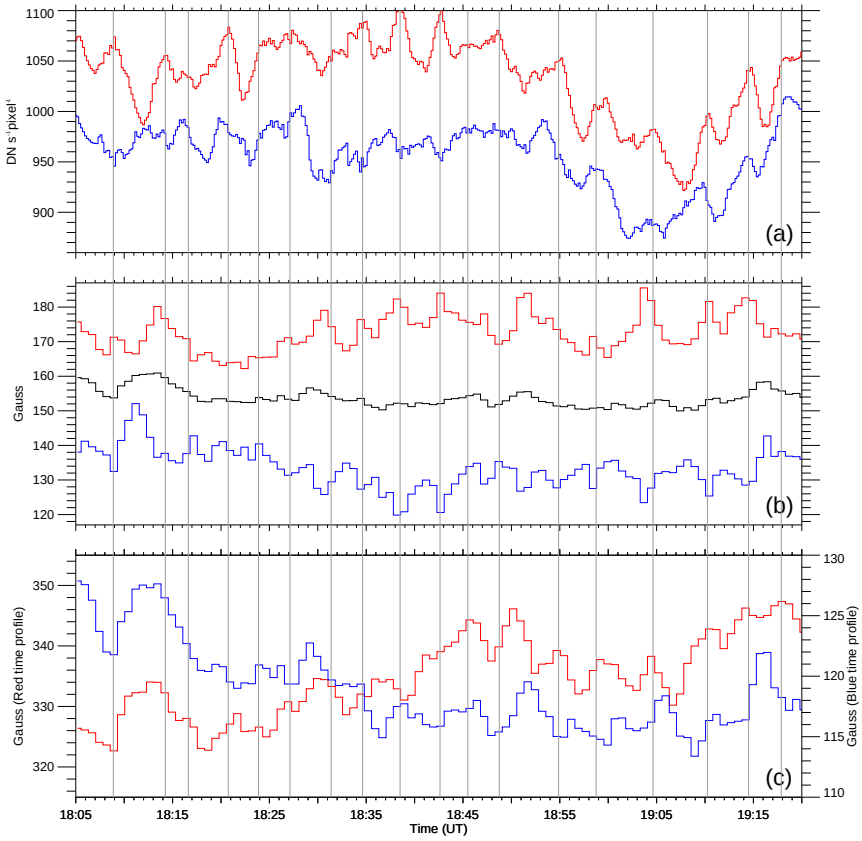

Fig. 4 Panels (a)-(b) feature two kinds of time profiles for the mean EUV 171 Å emission and mean magnetic field (unsigned) in the moss region, with the *red-colored light curve* over the EAPs and the *blue-colored light curve* over the other regions (i.e., LAPs). In panel (b), the *dark curve* in the middle is the time profile of unsigned magnetic field averaged over the whole moss region. The *red-* and *blue-colored light curves* in the lower panel are the time profiles for the mean unsigned magnetic field averaged over the stronger (greater than 250 G) and weaker (less than 250 G) magnetic field regions at 18:42:41 UT, respectively. *Vertical grey lines* run through peaks on the time profiles of the EUV emission over the EAPs.

– They are squirted out of the area around the intergranular lanes,
– They are accompanied by EUV brightening,
– They are associated with a stronger magnetic field.

In addition, the peaks on the time profile of the EUV emissions are found to be in sync with oscillatory peaks of the stronger magnetic field in the region. In our previous paper (Ji et al. 2021), we report that the magnetic perturbations are actually magneto-acoustic oscillations on the solar surface powered by the p-mode oscillation. For the two regions with the stronger and weaker magnetic field, the perturbations are frequently anti-phased. Therefore, signals of magnetic oscillations are usually reduced when the magnetic fluxes of the stronger field region and the weaker field region are integrated together. Only if we differentiate between the two kinds of regions can we identify obvious signals of magnetic oscillations, and thus find their correlation with EUV emissions.

All observations reported in this paper provide evidence supporting that coronal heating in the plage region is powered by magneto-acoustic oscillations or waves. The magneto-acoustic waves may turn into upward propagating shocks when they meet a sharp change in density (Hansteen et al. 2006; Rouppe van der Voort et al. 2016) or they may even modulate ongoing small-scale magnetic reconnection (Chen & Priest 2006; Samanta et al. 2019). The existence of Alfvén waves is worthy of further research incorporating detailed phase analysis for these magnetic perturbations. The observations seem to also support the magnetic gradient pumping (MGP) mechanism (Tan 2014). In the MGP mechanism, the magnetic gradient may drive energetic particles to move upward from the underlying solar atmosphere and form hot upflows. To determine which mechanism really works for coronal heating, current data are still insufficient in terms of spatial resolution, temporal cadence and spectral coverage. With current large-aperture solar telescopes (Cao et al. 2010; Goode et al. 2010; Liu et al. 2014), spectro-polarimetry observations with higher resolution and high-cadence for the interface layer will be especially helpful to finally resolve the problem of coronal heating.

Acknowledgements This work is supported by the National Natural Science Foundation of China (Grant Nos. 11333009, 11790302 (11790300), 11773061, 11729301, 11773072 and 11873027). We thank the SDO/AIA, and SDO/HMI teams for providing valuable data. SDO is a NASA project. The AIA and HMI data are downloaded via the Virtual Solar Observatory and the Joint Science Operations Center. BBSO operation is supported by NJIT and US NSF AGS-1821294 grant. GST operation is partly supported by the Korea Astronomy and Space Science Institute, the Seoul National University, and the Key Laboratory of Solar Activities of Chinese Academy of Sciences (CAS) and the Operation, Maintenance and Upgrading Fund of CAS for Astronomical Telescopes and Facility Instruments.

References

Aschwanden, M. J., Winebarger, A., Tsiklauri, D., et al. 2007, ApJ, 659, 1673
Banerjee, D., Erdélyi, R., et al. 2007, Sol. Phys., 246, 3
Berger, T. E., et al. 1999, ApJ, 519, L97
Cao, W., Gorceix, N., et al. 2010, Astronomische Nachrichten, 331, 636
Chen, P. F., & Priest, E. R. 2006, Solar Physics, 238, 313
De Pontieu, B., & Erdélyi, R. 2006, Phil. Trans. R. Soc. A, 364, 383
De Pontieu, B., Erdélyi, R., & de Wijn, A. G. 2003, ApJ, 595, L63
De Pontieu, B., McIntosh, S. W., Hansteen, V. H., et al. 2009, ApJ, 701, L1
De Pontieu B., Title, A. M., et al. 2014, Sol. Phys., 289, 2733
Dinesh Singh, H., & Singh Jatav, B. 2019, RAA (Research in Astronomy and Astrophysics), 19, 185
Fletcher, L., & De Pontieu, B. 1999, ApJ, 520, L135
Golub, L., Deluca, E., Austin, G., et al. 2007, Sol. Phys., 243, 63
Goode, P. R., Coulter, R., et al. 2010, Astron. Nachr., 331, 620
Hansteen, V. H., De Pontieu, B., Rouppe van der Voort, L., et al. 2006, ApJ, 647, L73
Hong, Z.-X., Yang, X., Wang, Y., et al. 2017, RAA (Research in Astronomy and Astrophysics), 17, 25
Jess, D. B., Morton, R. J., Verth, G., et al. 2015, Space Sci. Rev., 190, 103
Ji, H., Cao, W., & Goode, P. R. 2012, ApJ, 750, L25
Ji, H., et al. 2021, ApJ, submitted
Kolotkov, D. Y., Nakariakov, V. M., & Zavershinskii, D. I. 2019, A&A, 628, A133
Kosugi, T., Matsuzaki, K., et al. 2007, Sol. Phys., 243, 3
Li, Y. & Ding, M.-D. 2009, RAA (Research in Astronomy and Astrophysics), 9, 829
Liu, Z., Xu, J., Gu, B.-Z., et al. 2014, RAA (Research in Astronomy and Astrophysics), 14, 705
McIntosh, S. W., et al. 2011, Nature, 475, 477
Nakariakov, V. M., & Verwichte, E. 2005, Living Reviews in Solar Physics, 2, 3
Pesnell, W. D., Thompson, B. J., & Chamberlin, P. C. 2012, Sol. Phys., 275, 3
Peter, H., Tian, H., Curdt, W., et al. 2014, Science, 346, 1255726
Rouppe van der Voort, L., De Pontieu, B., Pereira, T. M. D., et al. 2016, ApJ, 799, L3
Samanta, T., Tian, H., et al. 2019, Science, 366, 890
Schou, J., Scherrer, P. H., et al. 2012, Sol. Phys., 275, 327
Stix, T. H. 1975, Nuclear Fusion, 15, 737
Tan, B. 2014, ApJ, 795, 140
Tian, H., DeLuca, E. E., Cranmer, S. R., et al. 2014, Science, 346, 1255711
Tian, H. 2017, RAA (Research in Astronomy and Astrophysics), 17, 110
Yang, X., Cao, W., Ji, H., et al. 2019, ApJL, 881, L25
Zeng, Z., Cao, W., & Ji, H. 2013, ApJL, 769, L33